Skin Research and Technology 2012; 18: 278–289
Printed in Singapore · All rights reserved
doi: 10.1111/j.1600-0846.2011.00562.x

Skin Research and Technology

Computer-aided pattern classification system for dermoscopy images

Qaisar Abbas[1], M. Emre Celebi[2] and Irene Fondón[3]

[1]Department of Computer Science, National Textile University, Faisalaba-37610, Pakistan, [2]Department of Computer Science, Louisiana State University, Shreveport, LA, USA and [3]Department of Signal Theory and Communications, School of Engineering Path of Discovery, Seville, Spain

Background: Computer-aided pattern classification of melanoma and other pigmented skin lesions is one of the most important tasks for clinical diagnosis. To differentiate between benign and malignant lesions, the extraction of color, architectural order, symmetry of pattern and homogeneity (CASH) is a challenging task.

Methods: In this article, a novel pattern classification system (PCS) based on the clinical CASH rule is presented to classify among six classes of patterns. The PCS system consists of the following five steps: transformation to the CIE *L*a*b** color space, pre-processing to enhance the tumor region and removal of hairs, tumor-area segmentation, color and texture feature extraction, and finally, classification based on a multi-class support vector machine.

Results: The PCS system is tested on a total of 180 dermoscopic images. To test the performance of the PCS diagnostic classifier, the area under the receiver operating characteristics curve (AUC) is utilized. The proposed classifier achieved a sensitivity of 91.64%, specificity of 94.14%, and AUC of 0.948.

Conclusion: The experimental results demonstrate that the proposed pattern classifier is highly accurate and classify between benign and malignant lesions into some extend. The PCS method is fully automatic and can accurately detect different patterns from dermoscopy images using color and texture properties. Additional pattern features can be included to investigate the impact of pattern classification based on the CASH rule.

Key words: melanoma – computer-aided diagnosis – dermoscopy – pattern recognition – texture analysis

Accepted for publication 7 July 2011

AUSTRALIA, NEWZEALAND, Japan, and U.S. are the most common countries known for their dry and sunny conditions having alarming rate of skin cancer, which is gradually increasing (1). Due to difficulty and subjectivity of visual interpretation of skin lesions, many dermatologists turn to computerized (2) image analysis techniques for dermoscopy images. In automated image analysis techniques, pre-processing, segmentation, and quantitation or description by the ABCD rule, pattern recognition by color, architectural order, symmetry of pattern and homogeneity (CASH) rule, and finally, classification (3) are common stages to classify pigmented skin lesions (PSLs). To categorize PSLs by dermoscopy, the most commonly used algorithms are pattern analysis; the ABCD rule of dermoscopy; the seven-point checklist; and the Menzies method (4). These clinical diagnosis rules are utilized by dermatologists to differentiate among skin lesions. Characteristic clinical features of early malignant melanoma, in general, can be described by 'ABCD', which stand for A = asymmetry, B = border irregularity, C = color variegation, which means that two or more colors exist within the tumor border, and D = diameter generally greater than 6 mm. To distinguish among tumors using ABCD rule and pattern classification methods, computer-aided diagnosis (CAD) tools are developed to increase the performance level of detecting skin lesions. The CAD systems (5, 6) provide screening support during followup assessments to dermatologists. For dermoscopy images, some automated melanoma classification systems (7–11) are developed using both clinical ABCD and pattern classification rules. The CAD of lesions using ABCD rule and pattern classification in dermoscopy images is challenging due to several

factors: (a) low contrast between the lesion and the surrounding skin, (b) hairs, (c) irregular and fuzzy lesion borders, (d) ineffective color and texture pattern extraction, and (e) variegated coloring inside the lesion. Among all these problems, an appropriate pattern classification remains as a challenging task for CAD systems. Therefore, to increase the performance level of CAD system, some studies have reported their pattern classification techniques.

Tanaka et al. (12) developed a method for pattern classification of nevus with texture analysis. The research was devoted to categorize three texture patterns: globular, reticular, and homogeneous patterns with 94% accuracy. Iyatomi et al. (13) developed melanocytic lesions classification system on acral volar skin with three pattern detectors, such as parallel ridge, furrow, and fibrillar patterns. They used more than 46 texture features with maximal value of between-class variance, and Mahalanobis generalized distance. Recently, in (14), a pattern analysis by color and texture features is modeled by Markov random field (MRF). In this study, mean and variance of each plane of CIE $L^*a^*b^*$ color space was used to extract the color-related features. For seven pattern classes, the authors reported 86% on average classification accuracy.

The literature review of pattern classification suggested that the researchers are more focused on extracting texture features, while less focus on color features. However, the authors have also reported that if tumor patterns are classified accurately, then to distinguish between benign and malignant melanomas become an easier task for the CAD system (12, 14).

To measure the texture patterns of tumors by taking into account the overall general appearance of CASH (15, 16) instead of clinical ABCD rule is also a challenging task for CAD tools. Using this method, physicians can classify between benign and malign lesions. The overall general appearance of CASH (17) is an important component in distinguishing these two groups. Hence, benign melanocytic lesions (18) tend to have few colors, an architectural order, symmetry of pattern and are homogeneous. Malignant melanoma often has many colors, architectural disorder, asymmetry of pattern, and is heterogeneous. In practice, the medical experts have mostly extracted seven texture patterns and measure uniformity to diagnosis of melanoma. In the benign lesion, the sizes and shape of patterns are uniformily distributed, whereas in melanoma, the size and shape of patterns are not uniform by location. Therefore, the pattern classification study can be used to differentiate between benign and melanoma tumors to some extend.

In this article, the computer-aided pattern classification system (PCS) based on CASH rule is presented using more focus on color and texture properties of lesions. Our PAC system consists of five consecutive steps: color space transforms, pre-processing and artifacts removal, segmentation, color and texture feature extraction, and finally, the classification decision is performed based on multiclass support vector machine (M-SVM) learning algorithm. In the color space transform step, first, RGB color dermoscopy image is changed to approximately uniform CIE $L^*a^*b^*$ color space (19). The tumor contrast is enhanced by homomorphic filtering (20) and hair artifact is then effectively repaired using our previous developed technique (21) based on derivative of Gaussian, morphologic functions, and fast marching techniques. After that, the tumor is segmented using skin tumor-area extraction (STEA) (22) technique. This segmentation method is based on an improved dynamic programming (IDP) approach. Next, the color and texture features are extracted for effectively utilizing CASH rule. First, the number of colors and their symmetry are determined. Second, the global and local texture feature interactions are determined by discrete wavelet frame (DWF) (23), and local binary pattern (LBP) (24), respectively. Third, a feature vector is constructed based on these features. Finally, the input pattern belongs to which class pattern is determined by M-SVM (25) based on the extracted color and texture properties. In this PCS study, the six different patterns, that is, Reticular: 30, Globular: 30, Cobblestone: 30, Homogeneous: 30, Parallel ridge: 30, and Starburst: 30, are obtained from a CD resource EDRA-CDROM, 2002 (26). For extracting and specifying patterns, we have requested an experienced dermatologist. According to diagnosis, location, age, gender, diameter and global feature, these patterns are arranged by this medical doctor. In this study, we classified six different patterns and exclude multicomponent pattern because in our classification protocol, each class pattern is matched with exactly one

class. The accuracy of pattern classification is measured by the area under the receiver operating characteristics (AUC) curve (27).

Materials and Methods

Dataset

The PCS system based on CASH rule is effectively applied on a total of 180 dermoscopy pigmented and non-pigmented skin lesions. This dataset was collected as a CD resource from the two European university hospitals as part of the EDRA-CDROM, 2002 (26). In total, this CD resource dataset consists of 1064 color dermoscopic images with spatial resolution of 768 × 512 pixels. All these images were captured during routine clinical assessments to imitate the *a priori* probabilities of the clinical diagnosis routine. For pattern PCS, we have requested a dermatologist to select and to arrange six classes of patterns according to diagnosis, location, age, gender, diameter, and global feature. Table 1 describes the average characteristics of age and diameter of each lesion and other features in this test dataset. The total 180 dermoscopic images of global features are selected of the following pattern categories: Reticular, Globular, Cobblestone, Homogeneous, Parallel ridge, and Starburst. Each pattern category is consisting of 30 images. In total, 20 melanoma lesions are presented in this dataset. Figure 1 shows one of the examples of each pattern present in our training dataset.

Method

Figure 2 shows the overall diagram of the proposed PCS, which includes color space transforms, pre-processing, tumor-area segmentation, color and texture feature extraction, and pattern classification stages. The subsequent paragraphs are describing the detailed information about the PCS system.

Color space transform

To segment tumor area, and extract color and texture features, a perceptually uniform color space is required. Specifically, distance measures must be correlated with perceived color differences and human visual system in the selected color space. The selection of color space is very important for classification task because color properties depend on a color difference formula, which must be uniform. In 1976, CIE presented two color spaces that approximately obsessed these characteristics, which are $L^*a^*b^*$ and $L^*u^*v^*$. Euclidean distances in those spaces were shown to be approximately correlated with perceptual color differences. Moreover, the white point adaptation present in the CIE $L^*u^*v^*$ system, with a subtractive shift instead of a multiplicative normalization, can result in poor visual correspondence and also in predicted corresponding colors lying outside the realizable gamut (19). Subsequently, the use of CIE $L^*a^*b^*$ should provide more accurate results than the ones obtained with the traditionally used color spaces, such as RGB or HSV because of its perceptual adaptation. Therefore, this perceptually adaptive color space was used in this study to accurately segment the skin color tumors and features extraction for effectively recognizing patterns. As a result, to pre-process or to segment tumor region, all RGB dermoscopy images were transformed to CIE $L^*a^*b^*$ color space.

Pre-processing

To facilitate the tumor-area segmentation algorithm and feature extraction steps, the uneven

TABLE 1. The selected dataset consists of a total of 180 dermoscopy images of six pattern classes and arrange according to age, gender, diameter, and diagnosis

	Attributes			
Global patterns	Age	Gender	Diameter	Diagnosis
Cobblestone pattern	34	Males:13 Females:17	9.45	CN:4, CMN:1, CON:3, DN:14, M :3, SB:2
Globular pattern	31.33	Males:22 Females:8	7.4	BCC:2, CN:28
Homogeneous pattern	91.13	Males:12 Females:18	9.7	BCC:3, BN:27
Parallel pattern	45.08	Males:19 Females:11	6.1	CN:30
Reticular pattern	35.37	Males:15 Females:15	7.2	CN:30
Starburst pattern	30.24	Males:12 Females:18	5.25	CN:3, M:6, RSN:21

BCC, basal cell carcinoma; BN, blue nevus; CMN, combined nevus; CN, Clark nevus; CON, congenital nevus; DN, dermal nevus; M, melanoma; RSN, Reed/Spitz nevus; SB, seborrheic keratosis.

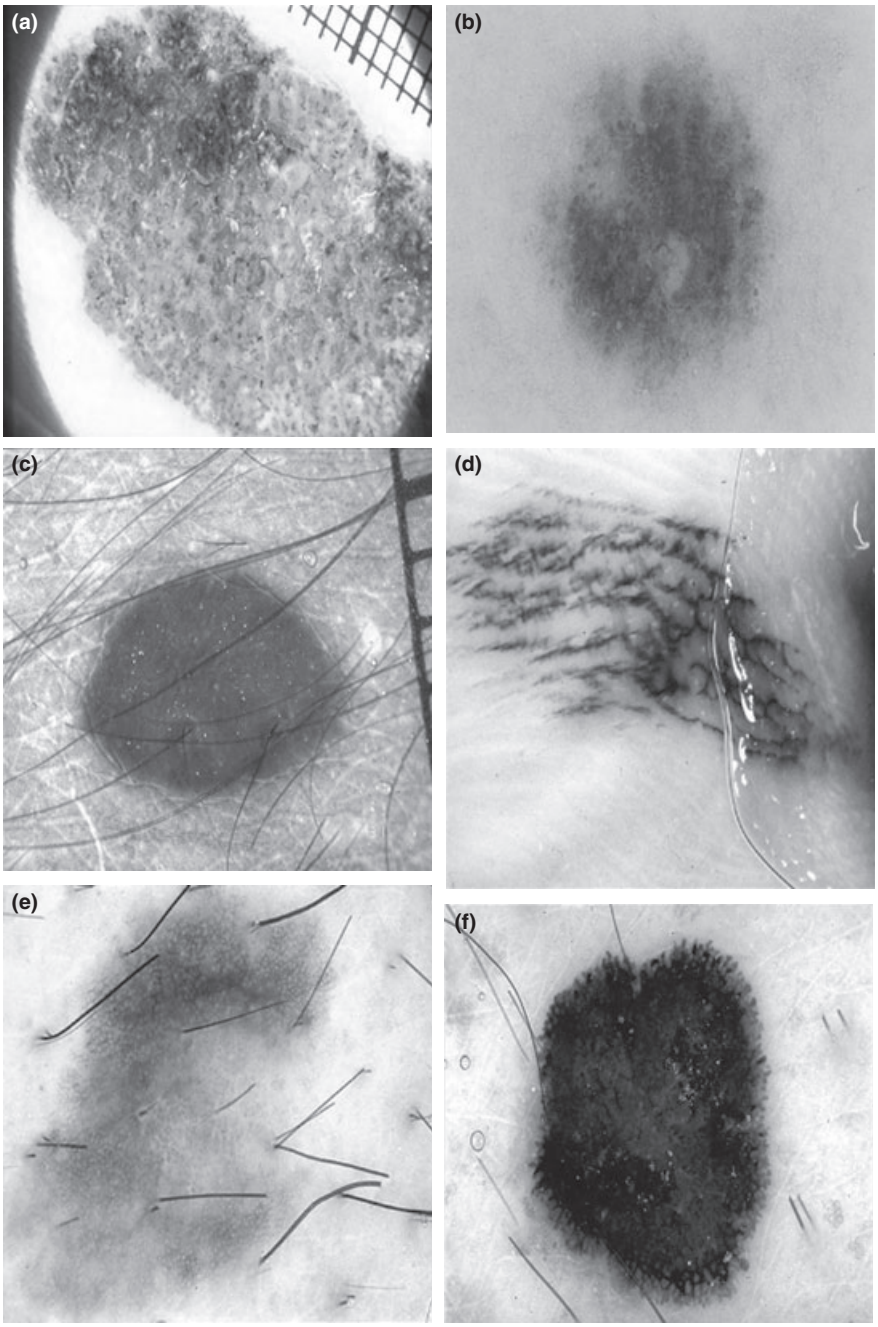

Fig. 1. Example of the different patterns present in dermoscopy images.

illumination correction and hair artifact repairing methods are performed.

As dermoscopic images are often affected by uneven illumination due to acquisition process, the homomorphic transform filtering (HTF) technique is utilized. To correct it, HTF method is applied on the luminance (L^*) plane of CIE $L^*a^*b^*$ color space. This step is described in detail in (20). Fundamentally, it is based on the idea that illumination and reflectance are combined through a multiplication operation to form an entire image. Applying logarithms to the expression, the relationship between illumination and reflectance becomes additive and thus, these two components of the image can be linearly separated in the frequency domain. As the illumination component tends to vary slowly across the image while the reflectance tends to change rapidly, the intensity variation across the image can be reduced while highlighting the details, considering high frequency components as reflectance and low frequency components as illumination, and then applying a high pass filter in the logarithmic domain. As

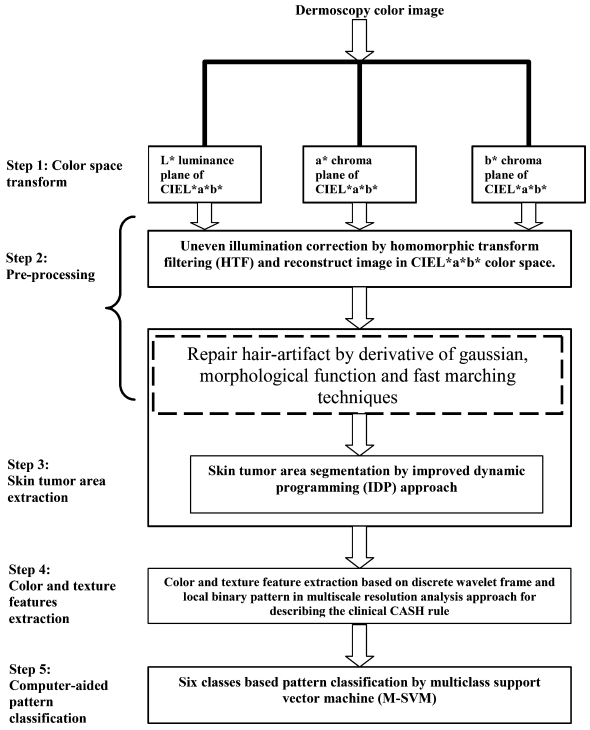

Fig. 2. Flow diagram of the proposed computer-aid-pattern classification system for dermoscopy images.

a result, an illumination corrected image is obtained. The illumination corrected image is shown in Fig. 3b of the parallel ridge pattern image.

The hair-pixels must be repaired from dermoscopy images without affecting tumors texture part. The hair-repairing step is one of the important steps before proceeding to next stage of segmentation or features extraction. In this study, the hair-repairing algorithm is used, which is based on derivative of Gaussian, morphologic function, and fast marching techniques that is described in this article (21). The hair detection is performed by 2D derivative of Gaussian (DOG) and morphologic functions. After that, the detected lines are repaired by 2D fast marching inpainting technique. Instead of exemplar-based inpainting, fast marching method was utilized because of its speed and effectiveness for noise repairing. This process is briefly described herein.

The hair-repair process is divided into three steps: hair detection with the use of a DOG, refinement by morphologic techniques and then hair repair by fast marching image inpainting technique. For detecting hair-like regions, we used luminance component of CIE *L*a*b** enhanced image and for repairing, all three components are utilized. To repair hair-occluded information from dermoscopy images, the fast and non-iterative inpainting method is utilized, which is developed by Bornemann and Marz. The inpainting technique utilize a fast marching method to traverse the inpainting domain while transporting the image values in a coherence direction by means of a structure tensor. Through the measure of the strength of

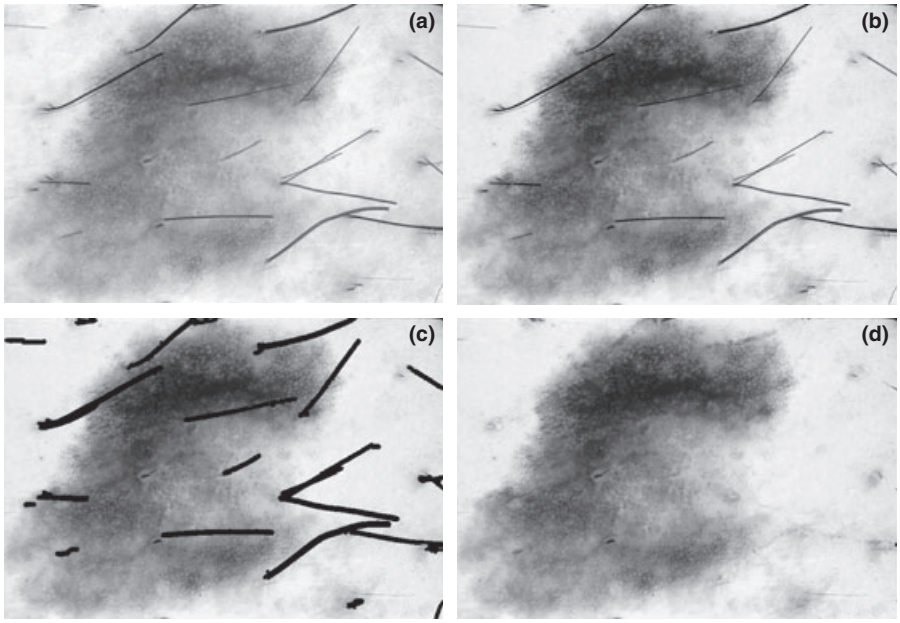

Fig. 3. Illumination correction and hair-pixels-repaired results of parallel ridge pattern dermoscopy image, which show (a) the original image, (b) illumination corrected, and (c) the hair-repaired one.

the coherence, this inpainting technique switches between diffusion and directional transport. By adding this robust coherence strength, the fast marching inpainting method is more effective than other inpainting methods, such as exemplar-based one. The results of hair detection and repairing steps are shown in Figs 3c and d.

Skin tumor-area extraction

After pre-processing skin images, the next step is to detect tumors' border. To extract color and texture features from tumors' area instead of other skin area, the STEA algorithm is followed, which is based on IDP (22). In this article, we have briefly introduced this segmentation technique and the interested reader may refer to (22) for more detailed information.

Initial segmentation is performed to get rough tumor segmented area of the luminance image (L^*) and is automatically segmented using minimum error thresholding method. Thus, an initial tumor area is detected, which is future utilized by IDP to refine this segmentation. As indicated before, the lesion's border is usually not clear, dim some part of tumor area, and also has an irregular shape. As a result, to detect these kind of blurred and uneven edges, an edge-based segmentation technique has been developed in CIE $L^*a^*b^*$ color space. To refine segmentation, we used edge-based approach that is computationally fast and do not need *a priori* information about the content of the image. However, the main problem of such kin of segmentation techniques is that it often fails to detect edges, when edges are not enclosing the object completely. Therefore, a post-processing step is always required to get the close-segmented boundaries. The dynamic programming (DP) techinque can be adopted in such situations to get closed boundaries and to reduce the complexity of the algorithm. In that STEA segmentation study, the DP techinque is improved to find out the optimal skin tumors area. The new local cost function was developed to IDP algorithm. In this IDP algorithm, the DP techinque is entirely implemented in taking account texture information using uniform color space. The IDP algorithm first calculated the radial profile from the center of the obtained initial segmented area of the lesion by transforming image Cartesian coordinates to polar coordinates. After that, a subsequent IDP procedure is applied to get an optimal path in this polar transform. An optimal path is calculated using the minimum cumulative cost matrix that can achieve the contour optimality step in the lesion extraction process. Finally, the Bezier-spline curve fitting technique is used to draw the smooth boundary from the local cost function. The whole STEA process is presented in Fig. 4.

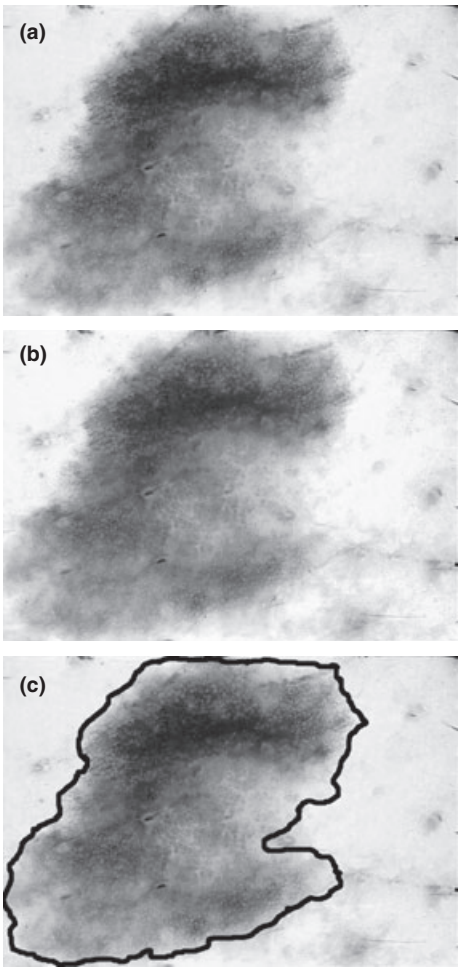

Fig. 4. The result of skin tumor-area extract (STEA) algorithm by an improved dynamic programming whereas (a) represents the pre-process image, (b) its luminance image, (c) segmented one.

Color and texture features extraction

From previous two steps, the enhanced tumor region is segmented, which is obtained without hair artifact. Next step is to extract the color and texture features from this segmented region. The color and texture features are providing important characteristics to quantitate the PSLs lesions. However, the literature studies focused more on extracting statistical properties

and hence, did not consider both local and global spatial correlated relationships among pixels. In case of parallel ridge and homogeneous patterns, it is very difficult to analyze texture by just considering global texture (14) properties. In addition to this, the color symmetry information is not considered in their approaches. Therefore, our classification system is based on both global and local spatial correlation among pixels and more focusing on color symmetry information, which are derived from color and texture features. Inspired by many color and texture features analysis studies (28–30), we have recognized that the color and texture features are used in a combine fashion to describe tumor patterns. To extract color-related features, we have calculated colors and their symmetry. After that, the texture features based on global and local pixels interactions are calculated on luminance (L^*) plane of CIE $L^*a^*b^*$ color space. Finally, the other planes (a^*, b^*) are also used to extract color-texture features.

For early diagnosis of PSLs, the extraction of color feature [6] plays a vital rule. For early diagnosis of melanoma and benign, the six shades of color and color symmetry are identified through dermoscopic imaging technique. The dermatologists have usually identified light-brown, dark-brown, white, red, blue, and black shades of color in PSLs tumors. To extract color features, first the spatially adaptive six shades of dominant colors are calculated in the segmented tumor regions. To measure the spatial adaptive dominant colors, we used the iterative k-means clustering algorithm with a fixed six number of clusters. In this clustering technique, every pixel of the image is represented by a color that is equal to the average color of the pixels in its neighborhood that belong to that class. This color composition feature representation consists of a number of locally adapted dominant colors and the corresponding percentage of occurrence (%occr) of each color within a certain neighborhood. After calculating colors with its percentage of occurrence, color symmetry of tumor regions are needed to calculate because it is an important measure of pigmented distribution in a certain neighborhood. To find out color symmetry, a technique based on perceived color differences is used that correspond to distances (#dist) among color pixels in CIE $L^*a^*b^*$ uniform color space. As a result, the color percentage ((%occr) and symmetric distance (#dist) attributes are used for the definition of color features.

To extract texture features, we used a DWF (23) approach that has multiresolution decomposition representation of texture information along with interesting translation and rotation invariance properties. In this features extraction step, we used two-level decomposition at 4-oriented scale for texture features extraction. On each decompose image, two types of features' vectors are constructed based on mean and variance. One is based on dominant energy features and the other is calculated by an LBP (24) operator.

To calculate dominant energy features, the global feature vector based on mean and variance energies of each subimage are calculated. This energy vector has sufficiently described the texture features because it indicates dominant spatial-frequency channels of the global pixels interaction. In this DWF feature extraction step, the mean and variance statistics measured are used to measure the energy of each subimage. We have extracted these statistical texture features from a sliding window (w) of size 16×16. If the segmented decomposed image is $I(m,n)$, where $1 \leq m \leq w$ and $1 \leq n \leq w$ such that M and N are the number of rows and columns, the energy function based on mean and variance is given by:

$$e_\mu(i,j) = 1/w^2 \sum_{m=1}^{w} \sum_{n=1}^{w} |I(m,n)| \tag{1}$$

and

$$e_\sigma(i,j) = 1/w^2 \sum_{m=1}^{w} \sum_{n=1}^{w} \left|I(m,n) - e_\mu(i,j)\right|^2 \tag{2}$$

As a result, the feature vector is constructed based on $e_\mu(i, j)$ and $e_\sigma(i, j)$ vector values of segmented image, $I(m,n)$ is then constructed by concatenating each block measure to make combined feature vector as:

$$f_{\mu,\sigma}^{\text{global}} = \cup_{i=1}^{k} \cup_{j=1}^{k_i} \left\{e_\mu(i,j), e_\sigma(i,j)\right\} \tag{3}$$

where, k is the number of DWF subbands and k_i is the number of blocks in the ith subband.

In addition to global pixels interaction, we have also calculated local interaction of pixels by means of LBP operator. The LBP operator is widely used for a gray scale invariant texture primitive statistic. For each pixel in an image, a

binary code is produced by thresholding a circularly symmetric neighborhood with the value of the center pixel. A histogram is created to collect the occurrences of different binary patterns. The basic version of the LBP operator considers only the eight-neighbors of a pixel, but the definition can be extended to include all circular neighborhoods with any number of pixels. By extending the neighborhood one can collect large-scale texture primitives. However, the eight-neighbors of a pixel are sufficient to describe local pixels interactions in each subband image of DWF transform.

To calculate local texture interactions, the LBP histogram approach is applied to each decomposed image. On each image, the mean $\mathrm{LBP}_{\mu}^{k_i}$ and variance $\mathrm{LBP}_{\sigma}^{k_i}$ of LBP histograms of sliding window (w) of size 16×16 are calculated to combine texture characteristics. The framework of texture feature extraction by means of DWF and LBP is represented in Fig. 5.

Finally, the mean value of each histogram is extracted.

$$f_{\mathrm{LBP}_{\mu,\sigma}}^{\mathrm{local}} = \cup_{i=1}^{k} \cup_{j=1}^{k_i} \left\{ \mathrm{LBP}_{\mu}^{k_i}, \mathrm{LBP}_{\sigma}^{k_i} \right\} \tag{4}$$

The feature vector constructed based on local and global pixels interaction of DWF transform of luminance (L^*) image can be used for effective patterns classification. However, the color-texture features based on chromacity (a^*, b^*) color information are also extracted in this classification study. We used mean and variance statistics of LBP histogram to obtained color-texture characteristics denoted by $\mathrm{LBP}_{\mu}^{a*,b*}$ and $\mathrm{LBP}_{\sigma}^{a*,b*}$, respectively. To extract color-texture features, the same sliding window of size 16×16 is used.

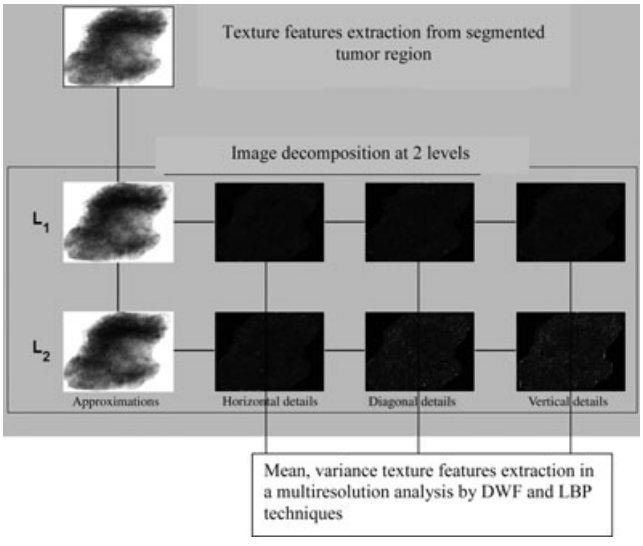

Fig. 5. The framework of the texture features extraction by discrete wavelet frame (DWF) and local binary pattern (LBP).

In total, the eight attributes' vectors are used to represent the color and texture feature, which is collectively written as:

$$f = \left\{ \%\mathrm{occr}, \#\mathrm{dist}, f_{\mu,\sigma}^{\mathrm{global}}, f_{\mathrm{LBP}_{\mu,\sigma}}^{\mathrm{local}}, \mathrm{LBP}_{\mu}^{k_i}, \mathrm{LBP}_{\sigma}^{k_i}, \mathrm{LBP}_{\mu}^{a*,b*}, \mathrm{LBP}_{\sigma}^{a*,b*} \right\} \tag{5}$$

Computer-aided pattern classification

The constructed feature vector of eight different attributes is used by M-SVM for training and testing of each pattern class. The optimized M-SVM (25) is used for final classification decision for matching the test pattern to which class. As mentioned earlier, we have 30 images of each six different pattern classes. Therefore, 80% images of six different classes are used for testing, whereas 20% of them are used for training the M-SVM classifier. For classification analysis, support vector machines (SVMs) are widely used that contain a set of related supervised learning methods to analyze data and to recognize patterns. In basic SVMs-based classification techniques, a binary classifier is constructed to make differentiation among two classes. However, we used M-SVM classifier for six pattern recognition in computer-aided classification of dermoscopy patterns.

The main objective of M-SVM is to allocate class labels to set of instances using SVMs. In practice, we are reducing the single multiclass approach to multiple binary classification problems using the M-SVM. The process of M-SVM is to produce a binary classifier of each problem that is considered an output function, which provides relatively large values from the positive class and small values from the negative class. In the literature, there are two approaches to build such binary classifiers for distinguishing, between one of the labels to the rest (one-vs.-all) or between every pair of classes (one-vs.-one). In this pattern classification study, we are using one-vs.-all strategy because the recognition of new instances for this strategy is done by a winning stage. In the winning stage, the new instance matches with the label to which the classifier is assigned the highest

output functions. In case of one-vs.-one, the recognition of new instances is done by majority voting scheme. Therefore, for dermoscopy pattern classification, the one-vs.-one approach is effectively sufficient for final classification decision.

Results and Discussion

The computer-aided-based PCS was tested on a total of 180 dermoscopy images with six different patterns, that is, Reticular (30), Globular (30), Cobblestone (30), Homogeneous (30), Parallel ridge (30), and Starburst (30). To do effective pattern classification, we first pre-process the 180 dermoscopy images to enhance the contrast by homomorphic transform filtering (HTF) and to remove hair-pixels by derivative of Gaussian, morphologic function and fast marching inpainting techniques. After that, an STAE algorithm is applied for delineated region of tumors only. Next, color and texture-related features are extracted to describe both local and global pixels interaction for effectively describing tumors' patterns. The feature vector is constructed based on eight different color and texture-related features of each tumor in the total 180, which is based on the CASH clinical rule. All the stages are performed in a perceptual uniform CIE $L^*a^*b^*$ color space. Finally, the classification decision of new test pattern is matched with the training instances using M-SVM machine learning algorithm. In the training of M-SVM, we used 80% tumor images, and 20% tumor images are used for testing the classifier accuracy.

To access the performance level of PCS system, the AUC (27) analysis is used to find out the sensitivity and specificity. The AUC is widely used to evaluate the overall classification results. It should be noticed that the AUC ranges from 0.5 to 1.0 and its higher value indicates the best classification accuracy.

The PCS algorithm was preliminarily implemented in Matlab 7.6.0.324® (The Mathworks, Natick, MA, USA). On average, the pre-processing step took in total 7.3 s for contrast enhancement and for hair repairing and 2.8 s to segment the lesion area by STEA. To extract color and texture features, on average 5.23 and 8.78 s are expended on each segmented tumor region for constructing the training and the testing dataset, respectively. Hence, for training the M-SVM classifier on this dataset, a total of 4.23 s is consumed for each pattern class. However, in case of testing a new pattern instance, on average 9.12 s is taken. For most part of the computation, time is spent on the feature extraction and training the M-SVM classifier for multiple class patterns. The computation time can be decreased by means of using optimized C/C++ implementation. All computations were executed on a 2.0 GHz Core to Duo 32-bit Intel processor with 1 GB DDR2 RAM, running Windows 7 Enterprise, Microsoft Corporation, USA.

TABLE 2. Performance measure of six different dermoscopy patterns along with melanoma classification using AUC curve

Pattern classification	Sensitivity	Specificity	AUC
Cobblestone pattern	91.70	93.60	0.941
Globular pattern	90.5	94.99	0.935
Homogeneous pattern	89.45	92.30	0.929
Parallel pattern	93.43	98.26	0.965
Reticular pattern	90.0	93.0	0.940
Starburst pattern	91.71	95.10	0.953
Melanoma	96.5	98.11	0.989

AUC, area under the receiver operating curve.

The classification results of proposed PCS system on the 180 dermoscopy dataset are presented in Table 2. In this table, the classification accuracy of each pattern class is measured in terms of sensitivity and specificity, and AUC measures. As displayed also in this table, it can be noticed that in case of Cobblestone, Parallel, Reticular, and Starburst patterns, the best performance have been measured, that is, AUC:

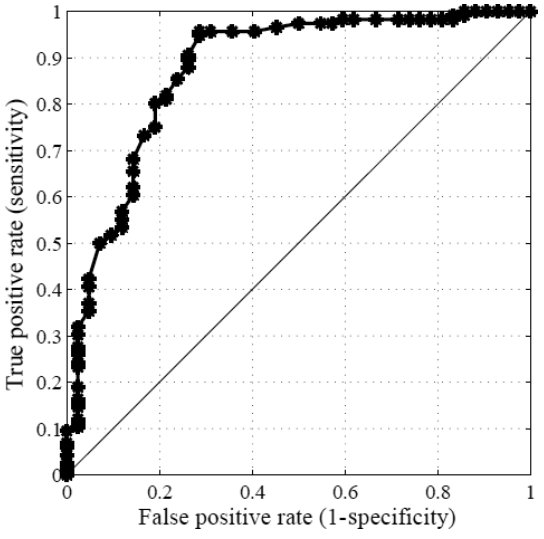

Fig. 6. Receiver operating characteristics (ROC) curve for the multi-class SVM learning algorithm on 180 dermoscopy images.

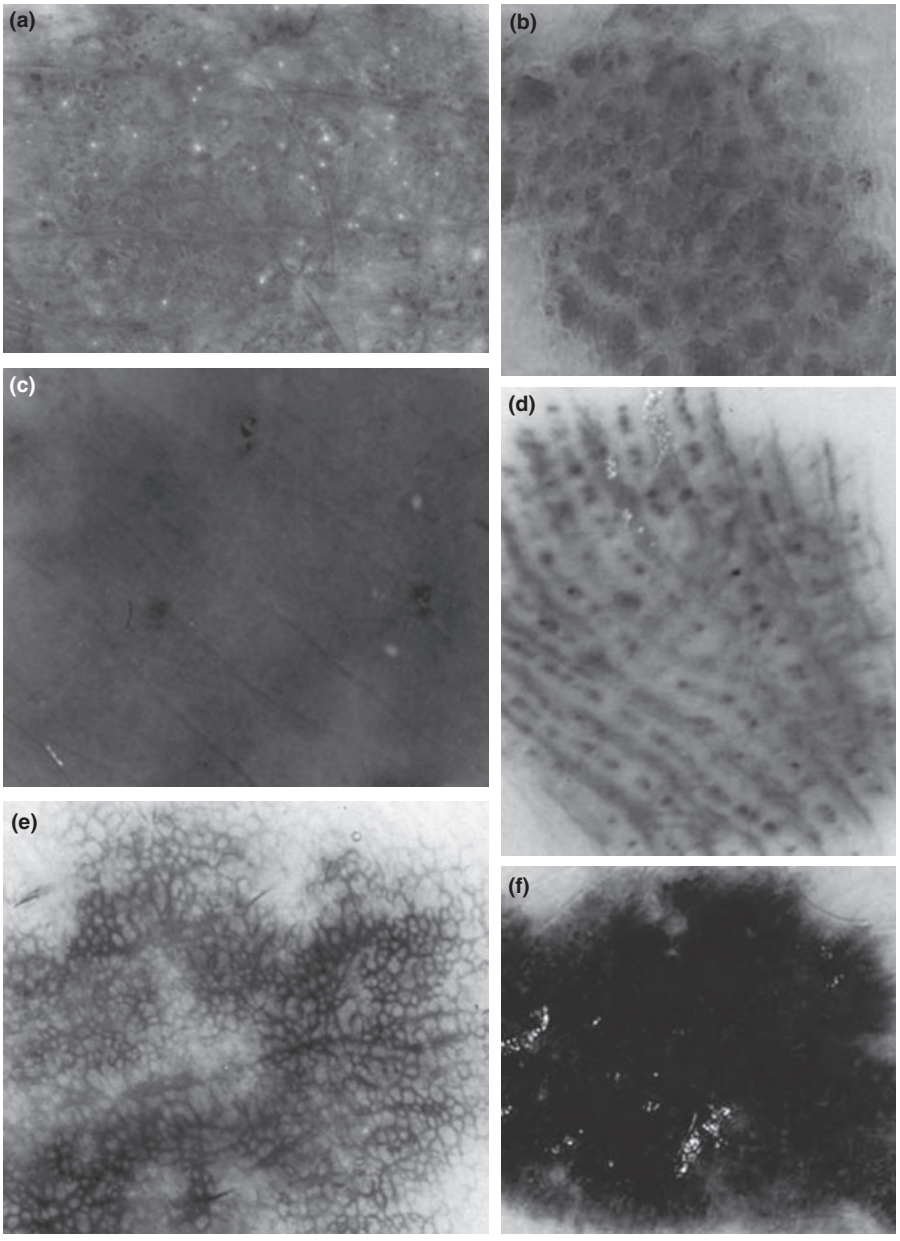

Fig. 7. Six different match pattern classes, where (a) cobblestone pattern, (b) globular pattern, (c) homogeneous pattern, (d) parallel pattern, (e) reticular pattern, and (f) starburst pattern.

0.941, AUC: 0.965, AUC: 0.940, and AUC: 0.953, respectively. Table 2 also presents the classification results of melanoma as compared to Clark nevus. For melanoma classification, the AUC area is 0.989. The greater the value of AUC, the higher is the classification accuracy. Figure 6 shows the corresponding receiving operating characteristic curve (ROC) of M-SVM machine learning algorithm in terms of six different pattern classes. Some of the sample dermoscopy images belonging to each class of pattern are shown in Fig. 7.

The main focus of this pattern classification study is to present an effective pattern detector technique for detection of skin lesions based on dermoscopy images. Color space transform, pre-processing, artifacts removal, lesion segmentation, the color and texture-related feature extraction, and final classification steps are integrated in a single system. If we combined this PAS with ABCD rule, then it could increase the performance level of computer-aided detection (CAD) of lesions or content-based image retrieval (CBIR) systems. As both CAD and CBIR

systems provide better presentation of results, an effective diagnosis system provides quick feedback to medical doctors for the 'screening support systems'.

The ABCD rule and pattern classification by CASH rule are common methods to decide, which category an input dermoscopy image belongs to, melanoma or other pigmented skin lesions, although CASH rule is one of the important components in distinguishing these two groups. The color and texture feature extractions are the key parameters in the description of regions of lesions. In general, multiscale feature extraction provides an effective solution for pattern analysis. Among multiscale features extraction algorithms, the global and local texture features extraction in multiscale are implemented in CIE $L^*a^*b^*$ uniform color space. As presented in the literature, many researchers have extracted patterns from luminance (L^*) plane of this uniform color space. On contrary, our feature extraction system has extracted color-texture features on all three planes of this color space to effectively measure the texture patterns. Therefore, our PCS is more robust than in the literature (14). It could be used to differentiate between benign and malignant tumors to some extend.

Conclusion

In this study, a novel PCS is proposed for dermoscopy images that can assist the dermatologists in a computer-based classification system. The main aim of this study was to develop and to test an effective PCS based on CASH clinical rule. Therefore, the proposed PCS system is developed, which focus more on color and texture features than the literature study (14). In the proposed PCS system, first, the color RGB images are transformed to CIE $L^*a^*b^*$ uniform color space. In the second step, the pre-processing operation is performed to enhance the contrast and to repair the hair pixels. The tumor segmentation step is then performed to get healthy tumor area as compared to surrounding skin. This segmented tumor area is then used to extract color and texture features based on color symmetry, texture features, and color and texture features combined. The feature vector is constructed based on these extracted properties of each tumor region. Finally, the M-SVM classifier is used to assess the discrimination of each pattern class on the total 180 dermoscopy images. From the overall discrimination performance of the proposed patterns classification model, we obtained an average sensitivity (SE): 93.08%, specificity (SP): 91.45%, and an AUC: 0.948 on a 180 dermoscopy dataset.

An accurate and automatic pattern analysis of melanocytic lesions and melanomas was critical for dermatologists to evaluate by clinical dermoscopic procedures (CASH) and to achieve results greater than 90%. Hence, this pattern discriminator based on color-texture features achieved higher classification accuracy. The proposed pattern classification method appears to be sufficiently accurate, robust, and computationally fast for discrimination of lesions, which helps the dermatologists in a 'screening support system' or in a CAD system. In the future work, we will add more global and local pattern classes to test its performance, and add more attributes to differentiate between benign and malignant tumors.

Acknowledgement

This study was supported by the Chinese Scholarship Council (CSC) (grant no. 2008GXZ143).

References

1. Coups EJ, Manne SL, Heckman CJ. Multiple skin cancer risk behaviors in the U.S. population. Am J Prev Med 2008; 34: 87–93.
2. Rigel DS, Russak J, Friedman R. The evolution of melanoma diagnosis: 25 years beyond the ABCDs. CA Cancer J Clin 2010; 60: 301–316.
3. Argenziano G, Soyer HP, Chimenti S et al. Dermoscopy of pigmented skin lesions: results of a consensus meeting via the Internet. J Am Acad Dermatol 2003; 48: 679–693.
4. Johr RH. Dermoscopy: alternative melanocytic algorithms—the ABCD rule of dermatoscopy, menzies scoring method, and 7-point checklist. Clin Dermatol 2002; 20: 240–247.
5. Perednia DA, Gaines JA, Rossum AC. Variability in physician assessment of lesions in cutaneous images and its implications for skin screening and computer-assisted diagnosis. Arch Dermatol 1992; 128: 357–364.
6. Celebi ME, Kingravi HA, Uddin B et al. A methodological approach to the classification of dermoscopy images. Comput Med Imag Grap 2007; 31: 362–373.
7. Maglogiannis I, Kosmopoulos DI. Computational vision systems for the detection of malignant melanoma. Oncol Rep 2006; 15: 1027–1032.

8. Tenenhaus A, Nkengne A, Horn JF, Serruys C, Giron A, Fertil B. Detection of melanoma from dermoscopic images of naevi acquired under uncontrolled conditions. Skin Res Technol 2009; 16: 73–80.
9. Wollina U, Burroni M, Torricelli R, Gilardi S et al. Digital dermoscopy in clinical practise: a three-centre analysis. Skin Res Technol 2007; 13: 133–142.
10. Rubegni P, Risulo M, Burroni M. Reply to digital dermoscopy analysis and Internet-based program for discrimination of pigmented skin lesion dermoscopic images. Br J Dermatol 2006; 154: 571–572.
11. She Z, Liu Y, Damatoa A. Combination of features from skin pattern and ABCD analysis for lesion classification. Skin Res Technol 2007; 13: 25–33.
12. Tanaka T, Torii S, Kabuta I, Shimizu K, Tanaka M. Pattern classification of nevus with texture analysis. IEEJ Transactions on Electrical and Electronic Engineering 2008; 3: 143–150.
13. Iyatomi H, Oka H, Celebi ME, Ogawa K, Argenziano G, Soyer HP, Koga H, Saida T et al. Computer-based classification of dermoscopy images of melanocytic lesions on acral volar skin. J Invest Dermatol 2008; 128: 2049–2054.
14. Serrano C, Acha B. Pattern analysis of dermoscopic images based on markov random fields. Pattern Recogn 2009; 42: 1052–1057.
15. Henning JS, Dusza SW, Wang SQ et al. The CASH (color, architecture, symmetry, and homogeneity) algorithm for dermoscopy. J Am Acad Dermatol 2007; 56: 45–52.
16. Henning JS, Stein JA, Yeung J, Dusza SW. CASH algorithm for dermoscopy revisited. Arch Dermatol 2008; 144: 554–555.
17. Zalaudek I, Docimo G, Argenziano G. Using dermoscopic criteria and patient-related factors for the management of pigmented melanocytic nevi. Arch Dermatol 2009; 145: 816–826.
18. Rubegni P, Sbano P, Burroni M, Cevenini G, Bocchi C, Severi FM et al. Melanocytic skin lesions and pregnancy: digital dermoscopy analysis. Skin Res Technol 2007; 13: 143–147.
19. Green P, MacDonald L. Color Engineering. Achieving Device Independent Colour. West Sussex, England: Wiley, 2003.
20. Abbas Q, Celebi ME, Fondon I, Rashid M. Lesion border detection in dermoscopy images using dynamic programming. Skin Res Technol 2011; 17: 91–100.
21. Abbas Q, Celebi ME, García IF. Hair removal methods: a comparative study for dermoscopy images. Biomedical Signal Processing and Control 2011 (in press).
22. Abbas Q, Celebi ME, García IF. Skin tumor area extraction using an improved dynamic programming approach. Skin Res Technol, 2011(in press).
23. Unser M. Texture classification and segmentation using wavelet frames. IEEE Trans Image Process 1995; 4: 1549–1560.
24. Ojala T, Pietikäinen M, Mäenpää TT. Multiresolution gray-scale and rotation invariant texture classification with local binary pattern. IEEE Trans on PAMI 2002; 24: 971–987.
25. Weston J, Watkins C. *Multi-class support vector machines in ESANN'99*, Brussels, 1999 (A Technical Report).
26. Argeniano G, Soyer PH, De VG, Carli P, Delfino M. Interactive atlas of dermoscopy CD-ROM, Milan, Italy: EDRA medical publishing and New media, 2002.
27. Bradley AP. The use of the area under the ROC curve in the evaluation of machine learning algorithms. Patern Recogn 1997; 30: 1145–1159.
28. Mojsilovic A, Kovacevic J, Kall D, Safranek R, Ganapathy S. Matching and retrieval based on the vocabulary and grammar of color patterns. IEEE Trans Image process 2000; 9: 38–54.
29. Mäenpää T, Pietikäinen M. Classification with color and texture: jointly or separately? Patern Recogn 2004; 37: 1629–1640.
30. Chen J, Pappas TN, Mojsilovic A, Rogowitz BE. Adaptive perceptual color-texture image segmentation. IEEE T Image process 2005; 4: 1524–1536.

Address:
Dr. Qaisar Abbas
Department of Computer Science
National Textile University
Faisalabad-37610
Pakistan
Tel: +92 41 9230081 Ext: 140
Fax: +92 41 9200764
e-mail: drqaisar@ntu.edu.pk,
qaisarabbasphd@gmail.com